AIAA JOURNAL
Vol. 32, No. 5, May 1994

General Strong Conservation Formulation of Navier-Stokes Equations in Nonorthogonal Curvilinear Coordinates

H. Q. Yang,* S. D. Habchi,† and A. J. Przekwas‡
CFD Research Corporation, Huntsville, Alabama 35805

The selection of primary dependent variables for the solution of Navier-Stokes equations in the curvilinear body-fitted coordinates is still an unsettled issue. Reported formulations with primitive variables involve contravariant velocity components, Cartesian components, and velocity projections, also known as resolutes. Most of the formulations result in a weak conservation form of the momentum equations which contain grid line curvature- and divergence-related Coriolis and centrifugal terms. This paper presents a general strong conservation formulation of the momentum equations allowing the flexibility in choosing the various forms of the velocity components as the dependent variables. Ambiguous issues relating geometrical topology and forms of governing equations are discussed and clarified. Computational results obtained with both strong and weak forms are presented and compared to known analytical/experimental data. The results confirm the soundness of the formulation.

Introduction

MOST practical fluid flows occur in complex geometrical configurations. For this reason, various formulations of the Navier-Stokes equations and their discretization for body-fitted coordinate (BFC) systems have been investigated in a pressure-based finite (control) volume framework.[1-10] There are several options in the grid arrangement and choice of dependent variables in the momentum equations. It is well known that the formulation of the Navier-Stokes (N-S) equations with Cartesian components as dependent variables[1,2,9] in the curvilinear coordinates retains a strong conservation form. On the other hand, formulating the N-S equations with other components, such as contravariant[3,5,8] and covariant components, or velocity projections (or resolutes)[7,10] along covariant or contravariant base vectors is known to have a weak conservation form. An interesting discussion on this subject has been provided by Shyy and Vu.[11]

In the strong conservation form of the N-S equations, all terms are expressed in terms of derivatives of the unknown vector components with respect to the independent variables. The virtue of this form is that it is possible to solve the equations by a variety of stable schemes and still obey physical conservation laws (such as mass, momentum, and energy laws).[12] Indeed, by a strong conservation form, the physical conservation laws are satisfied not only in each control volume but also in the whole computational domain. On the other hand, in the weak conservation form, the curvatures and divergences of the grid lines introduce extra source terms into the governing equations. These terms are analogous to the fictitious body forces which result from the use of a noninertial reference frame (such as centrifugal and Coriolis forces). These terms are very sensitive to the uniformity and skewness of the mesh distribution, and they can cause serious problems in the numerical accuracy. Most importantly, the satisfaction of physical conservation laws may be jeopardized. In the aerospace application of computational fluid dynamics, where external and compressible flows are usually of major interest, a formulation having strong conservation form can preserve freestream properties without any pollution due to grid skewness. Furthermore, it can satisfy the Rankine-Hugoniot condition for shocks and discontinuities, and therefore it possesses a better shock-capturing capability.

The objective of this paper is to provide a comparison between the strong and weak conservation forms of the N-S equations and to identify the inherent problems with the weak conservation form. Subsequently, a general formulation of the equations in the curvilinear coordinates is presented, which bears all strong conservation properties possessed by those with Cartesian components. The present technique is tailored for the pressure-based method since most of the density-based formulations use the Cartesian components. In the proposed technique, the differentiation operators are applied directly to the velocity vector itself, instead of velocity components. This eliminates numerical diffusion due to the skewness of a flow relative to grid lines. Furthermore, the present formulation has a clear, simple form, and it can be applied to the N-S equations with either contravariant, covariant, or even velocity projection as the dependent variable. In the limiting case, the one with the Cartesian component can be retrieved. The purpose of the paper is to present a formal and elegant form of the N-S equations in general curvilinear coordinates and to analyze and clarify the properties of weak and strong conservation forms. The ideas leading to the general strong conservation formulation are also illustrated.

Following the mathematical formulation section, several examples are used to demonstrate the soundness and success of the new technique. Here, all the examples are carried out with the velocity projection as the dependent variable. The successful application of the present technique for a formulation with a contravariant component as the dependent variable can be found in two-phase flow codes developed at CFD Research Corporation.[13] Therefore, the conclusion drawn can be equally applied to the other formulations with either covariant or contravariant components.

Basic Mathematical Formulation

The Navier-Stokes equations can be written in a vector form as

$$\frac{\partial \rho}{\partial t} + \nabla \cdot (\rho \boldsymbol{V}) = 0 \tag{1}$$

$$\frac{\partial (\rho \boldsymbol{V})}{\partial t} + \nabla \cdot (\rho \boldsymbol{V}\boldsymbol{V}) = -\nabla p + \nabla \cdot [\mu (\nabla \boldsymbol{V}) + \mu (\nabla \boldsymbol{V})^T] + \boldsymbol{S} \tag{2}$$

where ρ is density, $\boldsymbol{V}$ the velocity vector, $\nabla\cdot$ the divergence operator, ∇ the gradient operator, p the pressure, μ the dynamic viscosity, and $\boldsymbol{S}$ the source vector.

Presented as Paper 92-0187 at the AIAA 30th Aerospace Sciences Meeting, Reno, NV, Jan. 6–9, 1992; received March 1, 1993; revision received Sept. 17, 1993; accepted for publication Sept. 20, 1993.

*Group Leader/Research. Senior Member AIAA.
†Group Leader/Research. Member AIAA.
‡Vice President/Research. Senior Member AIAA.

Instead of tensor manipulation,[5,8] the present study seeks a direct transformation of the above equations from the Cartesian coordinates to the curvilinear coordinates. The subsequent discretization by the control volume practice is applied to obtain the final finite difference equations. To start with, let us denote the Cartesian coordinates as x_i and the curvilinear coordinates as ξ^i. The covariant base vector in the curvilinear coordinates $\boldsymbol{g}_i$ is related to the base vector in the Cartesian coordinates $\boldsymbol{I}_j$ by

$$\boldsymbol{g}_i = \frac{\partial x_j}{\partial \xi^i} \boldsymbol{I}_j \tag{3}$$

The corresponding unit base vector is given by

$$\boldsymbol{e}_i = \frac{\boldsymbol{g}_i}{h_i}, \quad h_i = \sqrt{\boldsymbol{g}_i \cdot \boldsymbol{g}_i} \quad \text{no summation on } i \tag{4}$$

Here, h_i is a scale factor. With the base vectors defined as noted, the vector operators of Eqs. (1) and (2) can be transformed from the Cartesian coordinates to the curvilinear coordinates through the following relations:
gradient:

$$\nabla\phi = \boldsymbol{g}^j \frac{\partial \phi}{\partial \xi^j} = J \frac{\partial}{\partial \xi^j}\left(\frac{\boldsymbol{g}^j}{J}\phi\right) \tag{5}$$

divergence:

$$\nabla \cdot \boldsymbol{V} = J \frac{\partial}{\partial \xi^j}\left(\frac{\boldsymbol{g}^j}{J} \cdot \boldsymbol{V}\right) \tag{6}$$

and Laplacian:

$$\nabla^2\phi = J \frac{\partial}{\partial \xi^j}\left(\frac{\boldsymbol{g}^j \cdot \boldsymbol{g}^k}{J} \frac{\partial \phi}{\partial \xi^k}\right) \tag{7}$$

where ϕ is a scalar quantity, $\boldsymbol{g}^j$ is the contravariant base vector, which satisfies

$$\boldsymbol{g}_i \cdot \boldsymbol{g}^j = \delta_i^j \tag{8}$$

δ is the Kronecker's delta, and J is the Jacobian of the transformation,

$$\frac{1}{J} = \frac{\partial (x_1, x_2, x_3)}{\partial (\xi^1, \xi^2, \xi^3)} \tag{9}$$

The preceding operators are sufficient to expand and differentiate scalar transport equations in the curvilinear coordinates. On the other hand, the vector quantity transport equation needs further elaboration. A vector (say velocity vector) can be expressed as:

$$\boldsymbol{V} = V^i \boldsymbol{g}_i = V_i \boldsymbol{g}^i \tag{10}$$

where V^i is the contravariant component of the velocity vector and V_i is the covariant component. They are nonphysical in that they contain a scale factor. For example, in polar coordinates, the scale factor for θ direction is r, so that $\boldsymbol{g}_\theta$ is $\boldsymbol{e}_\theta/r$, and the contravariant component is (rv_θ). Using a nonphysical component may lead to undesirable mesh sensitivity in the vicinity of singularity such as pole ($r = 0$). This explains why the velocity components were divided by the corresponding scale factors during tensor transformation.[5,8] It is, therefore, wise to use physical components which are denoted by a parenthesis in the index, $V^{(i)}$ and $V_{(i)}$:

$$\boldsymbol{V} = V^{(i)} \boldsymbol{e}_i = V_{(i)} \boldsymbol{e}^i \tag{11}$$

where

$$V^{(i)} = \frac{V^i}{h_i}, \quad V_{(i)} = \frac{V_i}{h^i} \tag{12}$$

with $\boldsymbol{e}^i$ as the unit contravariant base vector:

$$\boldsymbol{e}^i = \frac{\boldsymbol{g}^i}{h^i}, \quad h^i = \sqrt{\boldsymbol{g}^i \cdot \boldsymbol{g}^i} \text{ no summation on } i \tag{13}$$

A velocity projection (or resolute) can also be defined as

$$u_i = \boldsymbol{V} \cdot \boldsymbol{e}_i, \quad \text{or} \quad u^i = \boldsymbol{V} \cdot \boldsymbol{e}^i \tag{14}$$

Figure 1 shows the two-dimensional schematics of a velocity vector expressed in terms of physical contravariant and covariant components, as well as velocity projections. With the preceding relations the continuity equation can be transformed as

$$\frac{\partial}{\partial t}\left(\frac{\rho}{J}\right) + \frac{\partial}{\partial \xi^i}\left(\frac{\rho \boldsymbol{g}^i}{J} \cdot \boldsymbol{V}\right) = 0 \tag{15}$$

By virtue of Eq. (8):

$$V^i = \boldsymbol{V} \cdot \boldsymbol{g}^i, \quad V_i = \boldsymbol{V} \cdot \boldsymbol{g}_i \tag{16}$$

one can integrate Eq. (15) over a control volume surrounding node point P:

$$\frac{(\rho_p - \rho_p^o)\,\text{vol}}{\Delta t} + G_e^1 - G_w^1 + G_n^2 - G_s^2 + G_h^3 - G_l^3 = 0 \tag{17}$$

where

$$G_e^1 = (\rho V^{(1)} A^1)_e, \quad G_n^2 = (\rho V^{(2)} A^2)_n, \quad G_h^3 = (\rho V^{(3)} A^3)_h \tag{18}$$

A^i is the normal area to the ith direction, and vol is the volume. The subscripts e, w, n, s, h, and l represent the quantities at east, west, north, south, high, and low faces of the control volume. Depending on the temporal accuracy, G's can be evaluated at different time levels.

A similar procedure is applied to write the vector momentum equation in the curvilinear coordinates:

$$\frac{\partial}{\partial t}\left(\frac{\rho \boldsymbol{V}}{J}\right) + \frac{\partial}{\partial \xi^i}\left(\frac{\rho \boldsymbol{g}^i}{J} \cdot \boldsymbol{V}\boldsymbol{V}\right) = -\frac{\boldsymbol{g}^i}{J}\frac{\partial p}{\partial \xi^i} + \frac{\partial}{\partial \xi^i}\left(\mu \frac{\boldsymbol{g}^i \cdot \boldsymbol{g}^k}{J}\frac{\partial \boldsymbol{V}}{\partial \xi^k}\right)$$

$$+ \frac{\partial}{\partial \xi^i}\left(\mu \frac{\boldsymbol{g}^i}{J} \cdot \frac{\partial \boldsymbol{V}}{\partial \xi^k}\boldsymbol{g}^k\right) + \frac{\boldsymbol{S}}{J} \tag{19}$$

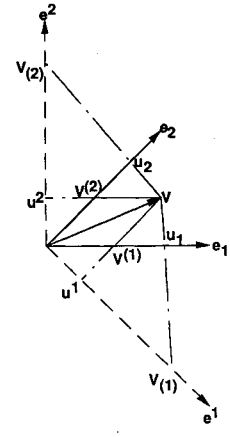

Fig. 1 Relationship between velocity resolutes (u_1, u_2, u^1, u^2), contravariant components ($v^{(1)}$, $v^{(2)}$), and covariant components ($v_{(1)}$, $v_{(2)}$).

To express the preceding equation in terms of the primitive variables (instead of the vector form), we can project the vector equation along a certain direction. This is accomplished by dotting (performing a dot product) the given momentum equation by a base vector $\boldsymbol{b}$. For demonstration purposes, we will only keep the transient, convective, and pressure gradient terms (Euler equation); the same procedure is applied to the diffusion terms except that it involves more tedious derivation. Now the Euler equation in Cartesian coordinates is transformed to [with relation (16)]

$$\frac{\partial}{\partial t}\left(\frac{\rho \boldsymbol{V}}{J}\right)+\frac{\partial}{\partial \xi^i}\left(\frac{\rho V^i}{J}\boldsymbol{V}\right)=-\frac{\boldsymbol{g}^i}{J}\frac{\partial p}{\partial \xi^i} \tag{20}$$

By dotting the above equation by $\boldsymbol{b}$, we have

$$\boldsymbol{b}\cdot\frac{\partial}{\partial t}\left(\frac{\rho \boldsymbol{V}}{J}\right)+\boldsymbol{b}\cdot\frac{\partial}{\partial \xi^i}\left(\frac{\rho V^i}{J}\boldsymbol{V}\right)=-\boldsymbol{b}\cdot\frac{\boldsymbol{g}^i}{J}\frac{\partial p}{\partial \xi^i} \tag{21}$$

The conventional transformation is done by bringing $\boldsymbol{b}$ into the differentiation on the left-hand side (LHS), so that Eq. (21) becomes:

$$\frac{\partial}{\partial t}\left(\frac{\rho \boldsymbol{V}\cdot\boldsymbol{b}}{J}\right)+\frac{\partial}{\partial \xi^i}\left(\frac{\rho V^i}{J}\boldsymbol{V}\cdot\boldsymbol{b}\right)-\frac{\partial \boldsymbol{b}}{\partial \xi^i}\cdot\frac{\rho V^i}{J}\boldsymbol{V}=-\boldsymbol{b}\cdot\frac{\boldsymbol{g}^i}{J}\frac{\partial p}{\partial \xi^i} \tag{22}$$

There are several interesting features associated with Eq. (22):

1) If $\boldsymbol{b}=\boldsymbol{I}_j$, the base vector in the Cartesian coordinates, the dependent variables are simply the Cartesian components, and the third term on the LHS of Eq. (22) is always zero. As a result, Eq. (22) is strongly conservative. This formulation has been used in Refs. 1, 2, and 9.

2) If $\boldsymbol{b}=\boldsymbol{g}^j$, the contravariant base vector in the curvilinear coordinates, the formulation is what has been derived by Demirdzic et al.[4] for two-dimensional and by Yang et al.[5,8] for three-dimensional curvilinear coordinates.

3) If $\boldsymbol{b}=\boldsymbol{g}_j$, the covariant base vector, the primitive variable in the momentum equation becomes the covariant component (V_i) of a velocity vector.

4) If $\boldsymbol{b}=\boldsymbol{e}_i$, the unit contravariant base vector, the primitive variable will be the velocity resolute, which is used by Parameswaran and Sun[7] and also in the PHOENICS code.[10]

Indeed, as long as $\boldsymbol{b}$ is a spatially variant base vector, Eq. (22) is always weakly conservative because of the existence of $\partial \boldsymbol{b}/\partial \xi^i$. Actually, by letting $\boldsymbol{b}=\boldsymbol{g}^j$ we can write Eq. (22) as

$$\frac{\partial}{\partial t}\left(\frac{\rho V^j}{J}\right)+\frac{\partial}{\partial \xi^i}\left(\frac{\rho V^i}{J}V^j\right)-\boldsymbol{g}_k\cdot\frac{\partial \boldsymbol{g}^j}{\partial \xi^i}\frac{V^iV^k}{J}=-\boldsymbol{g}^j\cdot\frac{\boldsymbol{g}^i}{J}\frac{\partial p}{\partial \xi^i} \tag{23}$$

where $\boldsymbol{g}_k\cdot\partial \boldsymbol{g}^j/\partial \xi^i$ is nothing but the Christoffell symbol of the second kind derived by tensor transformation.[5,8] It is due to this term that the momentum equation is weakly conservative.

To formulate an equation with $V_j=\boldsymbol{V}\cdot\boldsymbol{g}^j$, $V_j=\boldsymbol{V}\cdot\boldsymbol{g}_j$, or $u_i=\boldsymbol{V}\cdot\boldsymbol{e}_j$ as the dependent variable while at the same time ensuring the strong conservation property, we propose the following operation order, i.e., dotting Eq. (20) by $\boldsymbol{b}$ after the discretization. The idea of the proposed formulation comes from the observation that the momentum equation in the vector form [(Eq. 19)] is strongly conservative. Integration of Eq. (20) over a control volume yields the form:

$$\begin{aligned}&\frac{\left[(\rho \boldsymbol{V})_P-(\rho \boldsymbol{V})_P^o\right]\mathrm{vol}}{\Delta t}+(G\boldsymbol{V})_e^1-(G\boldsymbol{V})_w^1+(G\boldsymbol{V})_n^2-(G\boldsymbol{V})_s^2\\&+(G\boldsymbol{V})_h^3-(G\boldsymbol{V})_l^3=-A_P^1(\boldsymbol{e}^1)_P\,(p_e-p_w)\\&-A_P^2(\boldsymbol{e}^2)_P\,(p_n-p_s)-A_P^3(\boldsymbol{e}^3)_P\,(p_h-p_l)\end{aligned} \tag{24}$$

The approximation from a cell center to the cell face for the convective terms can be carried out as follows:

$$\begin{aligned}(G^1\boldsymbol{V})_e&=\frac{(G^1)_e}{2}(\boldsymbol{V}_E+\boldsymbol{V}_P)-\frac{\beta}{2}\left|(G^1)_e\right|(\boldsymbol{V}_E-\boldsymbol{V}_P)\\(G^1\boldsymbol{V})_w&=\frac{(G^1)_w}{2}(\boldsymbol{V}_W+\boldsymbol{V}_P)-\frac{\beta}{2}\left|(G^1)_w\right|(\boldsymbol{V}_P-\boldsymbol{V}_W)\\(G^2\boldsymbol{V})_n&=\frac{(G^2)_n}{2}(\boldsymbol{V}_N+\boldsymbol{V}_P)-\frac{\beta}{2}\left|(G^2)_n\right|(\boldsymbol{V}_N-\boldsymbol{V}_P)\\(G^2\boldsymbol{V})_s&=\frac{(G^2)_s}{2}(\boldsymbol{V}_S+\boldsymbol{V}_P)-\frac{\beta}{2}\left|(G^2)_s\right|(\boldsymbol{V}_P-\boldsymbol{V}_S)\\(G^3\boldsymbol{V})_h&=\frac{(G^3)_h}{2}(\boldsymbol{V}_H+\boldsymbol{V}_P)-\frac{\beta}{2}\left|(G^3)_h\right|(\boldsymbol{V}_H-\boldsymbol{V}_P)\\(G^3\boldsymbol{V})_l&=\frac{(G^3)_l}{2}(\boldsymbol{V}_L+\boldsymbol{V}_P)-\frac{\beta}{2}\left|(G^3)_l\right|(\boldsymbol{V}_P-\boldsymbol{V}_L)\end{aligned} \tag{25}$$

where β is a damping parameter, $0<\beta<1$. Note that when β is zero, the above approximation is equivalent to the second-order difference on the convective term, and when β is 1, it is the first-order upwind scheme. By substituting the above relation into Eq. (24) and making use of the continuity equation, we have

$$\begin{aligned}\left(a_p+\frac{\rho^o\mathrm{vol}}{\Delta t}\right)\boldsymbol{V}_P&=a_E\boldsymbol{V}_E+a_W\boldsymbol{V}_W+a_N\boldsymbol{V}_N+a_S\boldsymbol{V}_S\\&+a_H\boldsymbol{V}_H+a_L\boldsymbol{V}_L+\frac{\rho^o\mathrm{vol}}{\Delta t}\boldsymbol{V}_P^o-A_P^1(\boldsymbol{e}^1)_P\,(p_e-p_w)\\&-A_P^2(\boldsymbol{e}^2)_P\,(p_n-p_s)-A_P^3(\boldsymbol{e}^3)_P\,(p_h-p_l)\end{aligned} \tag{26}$$

where

$$\begin{aligned}a_p&=a_E+a_W+a_N+a_H+a_L\\a_E&=\tfrac{1}{2}\left[\beta\left|(G^1)_e\right|-(G^1)_e\right]\\a_W&=\tfrac{1}{2}\left[\beta\left|(G^1)_w\right|-(G^1)_w\right]\\a_N&=\tfrac{1}{2}\left[\beta\left|(G^2)_n\right|-(G^2)_n\right]\\a_S&=\tfrac{1}{2}\left[\beta\left|(G^2)_s\right|-(G^2)_s\right]\\a_H&=\tfrac{1}{2}\left[\beta\left|(G^3)_h\right|-(G^3)_h\right]\\a_L&=\tfrac{1}{2}\left[\beta\left|(G^3)_l\right|-(G^3)_l\right]\end{aligned} \tag{27}$$

At this point, Eq. (26) is strongly conservative since there are no grid curvature terms involved. This is the time to make a dot product of the preceding equation to choose primitive variables. As discussed earlier, there are several options:

1) Let $\boldsymbol{b}=\boldsymbol{I}_j$. The resultant primitive variable will be a Cartesian component, and the final equation is the same as used by the oth-

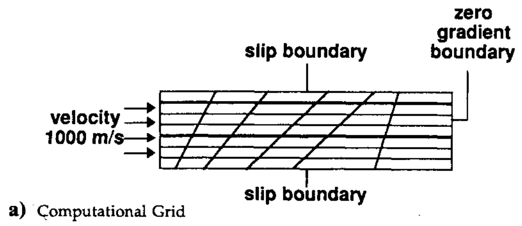

a) Computational Grid

1.00+E3	1.07+E3	9.93+E2	9.84+E2	9.85+E2	9.32+E2	9.51+E2
1.00+E3	1.02+E3	9.98+E2	9.99+E2	1.00+E3	9.78+E2	9.81+E2
1.00+E3	9.91+E2	9.78+E2	9.84+E2	9.86+E2	9.72+E2	9.83+E2
1.00+E3	9.69+E2	9.60+E2	9.70+E2	9.70+E2	9.66+E2	9.85+E2
1.00+E3	9.53+E2	9.44+E2	9.59+E2	9.59+E2	9.64+E2	9.89+E2
1.00+E3	9.38+E2	9.30+E2	9.55+E2	9.53+E2	9.70+E2	1.01+E3
1.00+E3	9.64+E2	9.98+E2	1.04+E3	1.05+E3	1.08+E3	1.10+E3

b) Predicted Axial Velocity (Weak Conservative Formulation)

1.00+E3	1.00+E3	1.00+E3	1.00+E3	1.00+E3	1.00+E3	1.00+E3
1.00+E3	1.00+E3	1.00+E3	1.00+E3	1.00+E3	1.00+E3	1.00+E3
1.00+E3	1.00+E3	1.00+E3	1.00+E3	1.00+E3	1.00+E3	1.00+E3
1.00+E3	1.00+E3	1.00+E3	1.00+E3	1.00+E3	1.00+E3	1.00+E3
1.00+E3	1.00+E3	1.00+E3	1.00+E3	1.00+E3	1.00+E3	1.00+E3
1.00+E3	1.00+E3	1.00+E3	1.00+E3	1.00+E3	1.00+E3	1.00+E3
1.00+E3	1.00+E3	1.00+E3	1.00+E3	1.00+E3	1.00+E3	1.00+E3

c) Predicted Axial Velocity (Strong Conservative Formulation)

Fig. 2 Computational grid and flow results for weakly conservative form.

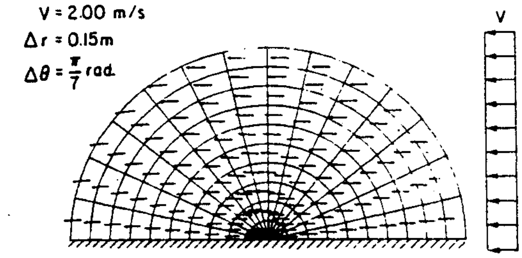

a) Grid and Boundary Conditions

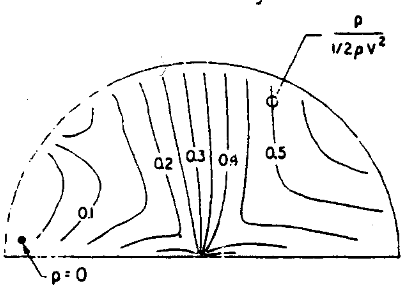

b) Weak Form, Pressure

Fig. 3 Inviscid incompressible flow through polar coordinate system; comparison of weak and strong conservative form.

ers.[1,2,9] The first drawback of this formulation is that cross pressure gradient terms are involved regardless of the grid being orthogonal or nonorthogonal as long as it is not Cartesian. This may introduce complexity in boundary conditions. The second drawback is that a transformation between the contravariant component used in the continuity equation and Cartesian component used in the momentum equation is required. However, this formulation has its appeal due to its simplicity.

2) Let $\boldsymbol{b} = (\boldsymbol{g}^j)_P$. The resultant primitive variable is the nonphysical contravariant component $(V^j)_P$.

3) An alternative to option 2 is to use $\boldsymbol{b} = (\boldsymbol{e}^j)_P$, the unit contravariant base vector. The primitive variable will be $V^{(j)}(\boldsymbol{e}_j \cdot \boldsymbol{e}^j)$ or simply the velocity projection along the $\boldsymbol{e}^j$ direction. The merit of this choice is that the physical contravariant component in the continuity equation (17) is the same as the primitive variable in the momentum equation, so that no transformation is needed. However, cross pressure gradient terms still exist.

4) Let $\boldsymbol{b} = (\boldsymbol{g}_j)_P$. Again, the resultant primitive variable is a nonphysical covariant component $(V^j)_P$.

5) An alternative to option 4 is to use $\boldsymbol{b} = (\boldsymbol{e}_i)_P$. Here the primitive variable is the velocity resolute or velocity projection along the $\boldsymbol{e}_i$ direction. It has the merit of single pressure gradient term for Eq. (26) when a staggered grid arrangement is used. However, the transformation between a resolute and a contravariant component is unavoidable.

Without loss of generality, we will use $\boldsymbol{b} = (\boldsymbol{e}^j)_P$ as an example, so that the primitive variable is the physical contravariant component, $V_P^{(j)}$. Realizing the following relation:

$$V_P \cdot (\boldsymbol{e}^j)_P = V_P^{(k)} (\boldsymbol{e}_k \cdot \boldsymbol{e}^j)_P \tag{28}$$

the dot product of Eq. (26) by $(\boldsymbol{e}^1)_P$ leads to:

$$\left(a_p + \frac{\rho^o \text{vol}}{\Delta t}\right) V_P^{(1)} = a'_E V_E^{(1)} + a'_W V_W^{(1)} + a'_N V_N^{(1)} + a'_S V_S^{(1)}$$
$$+ a'_H V_H^{(1)} + a'_L V_L^{(1)} + \frac{\rho^o \text{vol}}{\Delta t} (V_P^{(1)})^o - A_P^1 (p_e - p_w)(\boldsymbol{e}_1 \cdot \boldsymbol{e}^1)_P$$
$$- A_P^2 (\boldsymbol{e}^2 \cdot \boldsymbol{e}^1)_P \cdot (p_n - p_s) - A_P^3 (\boldsymbol{e}^3 \cdot \boldsymbol{e}^1)_P \cdot (p_h - p_l) + S' \tag{29}$$

where

$$a'_E = a_E (\boldsymbol{e}_1)_E \cdot (\boldsymbol{e}^1)_P, \quad a'_W = a_W (\boldsymbol{e}_1)_W \cdot (\boldsymbol{e}^1)_P$$
$$a'_N = a_N (\boldsymbol{e}_1)_N \cdot (\boldsymbol{e}^1)_P, \quad a'_S = a_S (\boldsymbol{e}_1)_S \cdot (\boldsymbol{e}^1)_P$$
$$a'_H = a_H (\boldsymbol{e}_1)_H \cdot (\boldsymbol{e}^1)_P, \quad a'_L = a_L (\boldsymbol{e}_1)_L \cdot (\boldsymbol{e}^1)_P \tag{30}$$

$$S' = \sum_{l = E, W, N, S, H, L} \left[a_l V_l^{(2)} (\boldsymbol{e}_2)_l \cdot (\boldsymbol{e}^1)_P + a_l V_l^{(3)} (\boldsymbol{e}_3)_l \cdot (\boldsymbol{e}^1)_P \right]$$

Equation (26) can be dotted with $(\boldsymbol{e}^2)_p$ and $(\boldsymbol{e}^3)_p$ using the preceding procedure to obtain equations for $V_P^{(2)}$ and $V_P^{(3)}$.

The diffusion terms can be approximated by the second-order central difference scheme, while the SIMPLE algorithm[14] can be used for velocity-pressure coupling, and pressure oscillation can be avoided by the use of the staggered grid.

In the next section, selected flow problems illustrate the difference between the weak and strong conservation forms. Accuracy of the proposed BFC formulation is demonstrated with selected CFD benchmark flow problems. Both strongly and weakly conservative formulations with velocity resolute as a dependent variable were incorporated into a CFD code, REFLEQS,[15] which was used for the present computations.

Computational Results

Inviscid Channel Flow

The first test case considered is a uniform inviscid flow through a rectangular channel. In this generic case the computational grid is composed of only six cells in the axial direction and six cells in the vertical direction, with highly skewed grid lines as shown in Fig. 2a. The velocity in each cell should equal the inlet velocity if no BFC numerical error is present. The inlet velocity is specified as 1000 m/s (304.8 ft/s), corresponding to a Mach number of 2.88 for 300 K (80°F) air. The expected correct solution should yield 1000 m/s everywhere in the domain.

Figure 2b shows that the weak conservation formulation gives about 10% error, and the velocity distribution in the channel is not

Table 1 Drag coefficients comparison

	C_p	C_f	C_d
Present weak form	0.8731	0.6258	1.4989
Present strong form	1.2118	0.7966	2.0084
Reference 16	1.201	0.794	1.995
Reference 17			2.0001

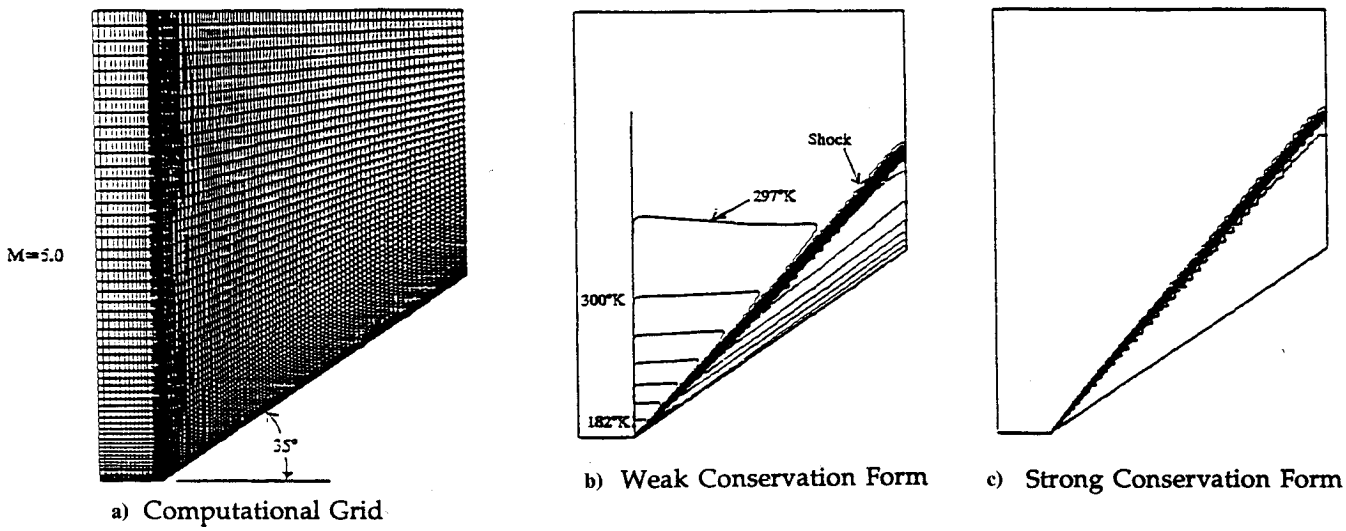

Fig. 4 Grid and temperature contours for supersonic flow over a 35-deg wedge.

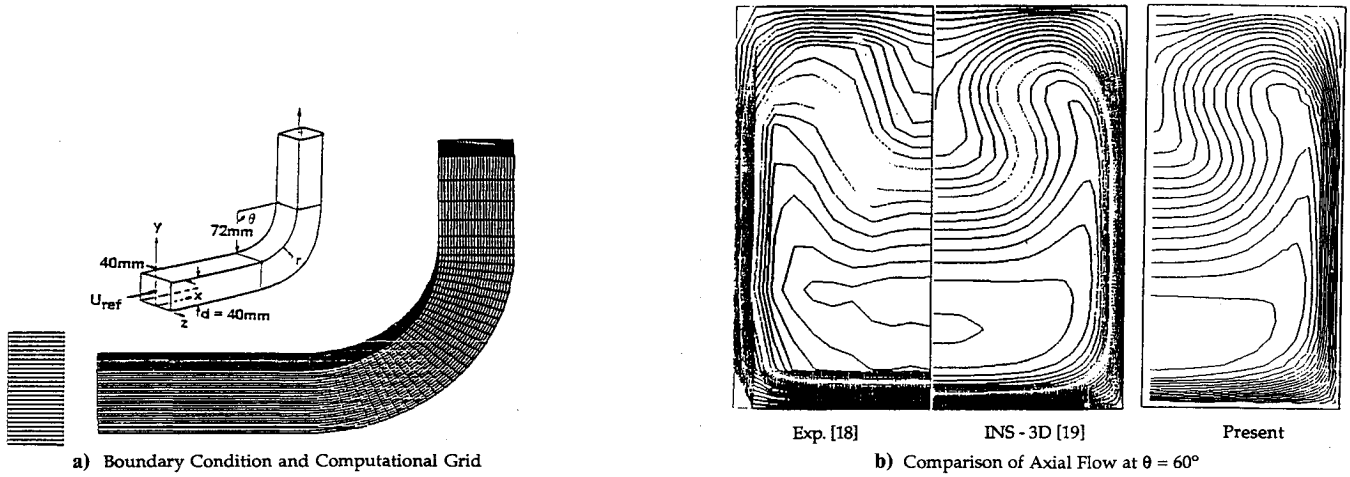

a) Boundary Condition and Computational Grid

b) Comparison of Axial Flow at θ = 60°

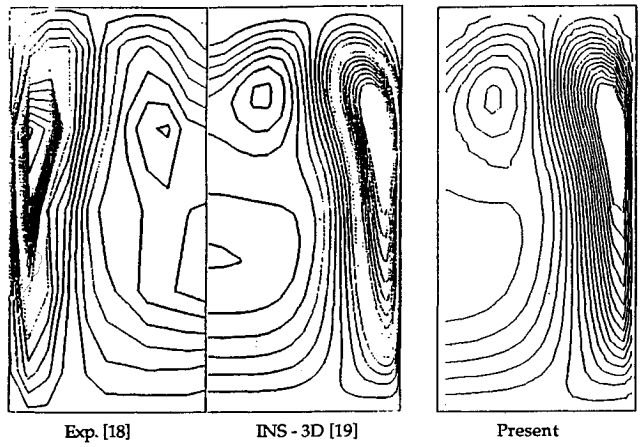

c) Comparison of Radial Flow at θ = 60°

Fig. 5 Flow in three-dimensional 90-deg bend square duct.

uniform. Apparently, the change of the coordinate line η with ξ gives rise to the centrifugal and Coriolis-type body forces so that the momentum equation cannot be satisfied for a simple uniform flow due to the unbalanced flow-geometric relations. The results obtained with the proposed formulation, with the same velocity projection as dependent variable, show a perfect flow distribution (Fig. 2c).

Inviscid and Viscous Incompressible External Flows

The second problem considers a uniform subsonic flow passing from right to left across a circular grid (Fig. 3a). Since the bottom surface is chosen as a symmetric plane, the correct solution is zero pressure loss and a uniform velocity. N-S equations in the polar coordinates expressed in terms of radial (V_r) and circumferential (V_θ) velocity components have a weakly conservative form with familiar centrifugal and Coriolis terms. Figure 3b presents the typical pressure distribution obtained with this form of the N-S equations.[3] Galpin et al.[3] attributed this to the enigmatic numerical diffusion error due to grid curvature, when flow is not aligned with the grid lines. With the present formulation (still with V_r and V_θ as the dependent variables), the solution is perfect. This proves the freestream preserving property of the present formulation.

Another external flow problem involves viscous flow through a cylinder of radius R. Here the results can be compared with those previously published.[16,17] For this free boundary problem, the outer boundary radius is chosen as 200 R to eliminate the influence of the far field. The cylinder surface is described as nonslip. The important parameter of the present problem is the drag coefficient (C_d) due to pressure (C_p) and friction (C_f). A 100 × 80 nonuniformly distributed grid is clustered near the cylinder surface to resolve the possible boundary layer. At a Reynolds number of 20 and $\beta = 0.001$, the computed drag coefficients are listed in Table 1. The results from Ingham and Tang[16] and from Fornberg[17] are also provided.

It is seen that the drag coefficients calculated by the present strong conservation formulation are in excellent agreement with those of Refs. 16 and 17. On the other hand, with a weak conservation form, the predicted drag coefficients are totally unacceptable.

Supersonic Flow Over a Wedge

To demonstrate the superior shock-capturing capabilities of the strong conservative form, a supersonic flow ($M = 5$) over a 35-deg wedge is considered. Figure 4a shows the120 × 60 computational grid used for this problem. Note that across the wedge starting line where sudden change in grid line angle exists, both Coriolis and centrifugal terms will appear in the weak conservation form of the N-S equations. Figures 4b and 4c present the temperature contours obtained with weak and strong forms. It is directly seen that the weakly conservative form gives large temperature (also pressure) spikes at the wedge. On the other hand, the strong conservative-form yields a sharp resolution of the oblique shock and correct reflection angle.

Incompressible Viscous Flow in a Three-Dimensional 90-Degree Bend Duct

The last problem compares the present formulation (with velocity projections as dependent variables) with another formulation that uses the Cartesian components as the dependent variables. The problem definition and computational grid are given in Fig. 5a. For the secondary flow, the experimental data by Taylor et al.[18] and numerical calculation by McConnaughey et al.[19] using incompressible Navier-Stokes (INS-3D) code, as well as the present calculation are shown in Figs. 5b and 5c. It is seen that the present calculation compares very well with experiments and the calculation obtained with the INS-3D code.

Conclusions

Traditional N-S formulation with non-Cartesian components as primitive variables cannot preserve freestream properties. When applied to supersonic flows, the formulation leads to spurious oscillations near shocks. The present paper proposes a general strong conservation formulation for the N-S equations, which can not only preserve freestream properties but also possesses excellent shock-capturing capabilities. The idea is to integrate the vector form of the momentum equation first and then decompose it into selected velocity components. In the classical approach these steps are reversed. The demonstration and validation examples show that the present formulation is robust and accurate for a wide class of problems from inviscid to viscous flows and from incompressible to highly compressible flows.

Acknowledgment

The authors wish to express their appreciation to S. Shea and J. Swann for their preparation of the typescript.

References

[1]Rhie, C. M., and Chow, W. L., "Numerical Study of the Turbulent Flow Past an Airfoil with Trailing Edge Separation," *AIAA Journal*, Vol. 21, No. 11, 1983, pp. 1525–1532.

[2]Shyy, W., Tong, S. S., and Correa, S. M., "Numerical Recirculating Flow Calculation Using a Body-Fitted Coordinate System," *Numerical Heat Transfer*, Vol. 8, No. 1, 1985, pp. 99–113.

[3]Galpin, P. F., Raithby, G. D., and Van Doormal, J. P., "Discussion of Upstream-Weighted Advection Approximation of Curved Grid," *Numerical Heat Transfer*, Vol. 9, No. 2, 1986, pp. 241–246.

[4]Demirdzic, I., Gosman, A. D., Issa, R. I., and Peric, M., "A Calculation Procedure for Turbulent Flow in Complex Geometries," *Computers and Fluids*, Vol. 15, No. 3, 1987.

[5]Yang, H. Q., Yang, K. T., and Lloyd, J. R., "Buoyant Flow Calculations with Non-Orthogonal Curvilinear Coordinates for Vertical and Horizontal Parallelepiped Enclosures," *International Journal for Numerical Methods in Engineering*, Vol. 25, No. 2, 1988, pp. 331–345.

[6]Karki, K. C., and Patankar, S. V., "Pressure Based Calculation Procedure for Viscous Flows at All Speeds in Arbitrary Configuration," *AIAA Journal*, Vol. 27, No. 9, 1989, pp. 1167–1174.

[7]Parameswaran, S., and Sun, R., "Numerical Aerodynamic Simulation of Turbulent Flows Around a Car-Like Body Using the Nonstaggered Grid System," AIAA Paper 89-1884, Jan. 1989.

[8]Yank, H. Q., Yang, K. T., and Lloyd, J. R., "A Control Volume Finite-Difference Method for Buoyant Flow in Three-Dimensional Curvilinear Non-Orthogonal Coordinates," *International Journal for Numerical Methods in Fluids*, Vol. 10, No. 2, 1990, pp. 199–211.

[9]Jiang, Y., Chen, C. P., and Chyu, M. K., "A Numerical Computation of Convective Heat Transfer in Two-Pass Rectangular Channels with a 180-Degree Sharp Turn," AIAA Paper 90-0355, Jan. 1990.

[10]Galea, E. R., and Markatos, N. C., "The Mathematical Modelling and Computer Simulation of Fire Development in Aircraft," *International Journal of Heat Mass Transfer*, Vol. 34, No. 1, 1991, pp. 181–197.

[11]Shyy, W., and Vu, T. C., "On the Adoption of Velocity Variable and Grid System for Fluid Flow Computation in Curvilinear Coordinates," *Journal of Computational Physics*, Vol. 92, No. 1, 1991, pp. 82–105.

[12]Vinokur, M.,"Conservation Equations of Gas Dynamics in Curvilinear Coordinate Systems," *Journal of Computational Physics*, Vol. 14, No. 2, 1974, pp. 105–125.

[13]Dionne, P. J., Budden, M. J., and Singhal, A. K., *Two-Phase: A Computer Program for Multi-Dimensional Two-Phase Flow Analysis of Riser/Separator Systems of Steam Generators, Volume 2: Theory Manual, Version 1.0*, CFD Research Corp., 4030/8, Huntsville, AL, March 1991.

[14]Patankar, S. V., *Numerical Heat Transfer and Fluid Flow*, Hemisphere, Washington, DC, 1980, Chap. 6.

[15]Przekwas, A. J., Habchi, S. D., Yang, H. Q., Avva, R. K., Talpallikar, M. V., and Krishnan, A., *REFLEQS-2D: Computer Program for Turbulent Flows with and without Chemical Reaction, Volume 1: User's Manual*, CFD Research Corp., GR-88-4, Huntsville, AL, Jan. 1990.

[16]Ingham, D. B., and Tang, T., "A Numerical Investigation into the Steady Flow Past a Rotating Circular Cylinder at Low and Intermediate Reynolds Numbers," *Journal of Computational Physics*, Vol. 87, No. 1, 1990, pp. 91–107.

[17]Fornberg, B., "Steady Viscous Flow past a Circular Cylinder up to Reynolds Number 600," *Journal of Computational Physics*, Vol. 6, No. 2, 1985, pp. 293–320.

[18]Taylor, A. M., Whitelaw, K. P., and Yianneskis, M., "Measurement of Laminar and Turbulent Flow in a Curved Duct with Inlet Boundary Layers," NASA Rept. 3307, Jan. 1981.

[19]McConnaughey, P., Cornelison, J., and Barker, J., "The Prediction of Secondary Flow in Curved Ducts of Square Cross-Section," AIAA Paper 89-0276, Jan. 1989.